Cement & Concrete Composites 33 (2011) 444–448

Contents lists available at ScienceDirect

Cement & Concrete Composites

journal homepage: www.elsevier.com/locate/cemconcomp

Nonlinear conduction in carbon fiber reinforced cement mortar

Jing Xu *, Wu Yao, Ruiqing Wang

Key Laboratory of Advanced Civil Engineering Materials (Tongji University), Ministry of Education, Shanghai 200092, China

ARTICLE INFO

Article history:
Received 27 February 2008
Received in revised form 9 October 2010
Accepted 14 October 2010
Available online 20 October 2010

Keywords:
Carbon fiber
Cement composite
Nonlinear behavior
Tunneling effect
Percolation theory

ABSTRACT

The present work regards the nonlinear electrical behavior of carbon fiber reinforced cement mortar in the dry state while the fiber content is near the percolation threshold. Tunneling effect theory and Ohm's law were employed to interpret the conductive mechanism. An obvious flat zone was observed in the resistivity–voltage plot when applied voltage is low. The critical voltage beyond which the resistivity starts to deviate differs with varying fiber volume fractions. A mathematical model relating resistivity of cement-based composite and the electric field intensity was validated experimentally. Fitting results show that the influence of tunneling effect on the conductivity of the system decreases significantly owing to the increasing fiber content. Consequently, tunneling barrier is no longer a hindrance to the motion of charge carriers when fiber content is in the vicinity or above the percolation threshold.

1. Introduction

Nonlinear current–voltage (*I*–*V*) behavior is common in a variety of materials, including semiconducting ceramics, conductive polymers, insulator/metal oxide junctions, etc. [1–3]. Tunneling effect is one of the main causes of this phenomenon, due to tunnel transmission of charge carriers at the interface of conductive phase and non-conductive phase [4,5]. As a multi-phase composite material, carbon fiber reinforced cement mortar (CFRC) is composed of conductive fibers and non-conductive cement matrix. It is reasonable to expect the nonlinear *I*–*V* behavior of CFRC, for tunnel paths between adjacent fibers are present [6].

The conductivity of CFRC in the applied electric field has been investigated much in previous research [7–9]. Electrical conduction in CFRC involves electrons and ions. In the water saturated state, ionic conduction dominates; whereas in the dry state, electronic conduction is more significant than ionic conduction [10]. Carbon fiber is an electronic conductor and the charger carriers would be electrons and/or holes. While in the dry state, two theories are usually employed to interpret the conduction mechanism of CFRC — one is percolation theory and the other is tunneling effect theory. An idealized model of percolation is that adjacent fibers physically contact and form a geometrically connected phase when the fiber content is near or above the percolation threshold. However, the tunneling effect also contributes to the conduction for the case when two adjacent fibers are not physically in contact, even when the fiber content is below the percolation threshold. In general, a low volume fraction of fibers (usually near the percolation threshold) is preferred in practice not only since lower cost, good workability and higher compressive strength (low air void content) can be obtained, but also a decrease of fiber addition close to the percolation threshold will increase the sensitivity of CFRC as a strain sensor [11]. Therefore, it is valuable to study the conductive behavior of CFRC near the percolation threshold.

Although there are many experimental results on the electrical performance of CFRC, numerical study is limited. Numerical simulation is important for a fundamental understanding of the conductive mechanism and a model of the phenomenon facilitates practical implementation. The objective of this paper is to investigate the nonlinear electrical behavior of CFRC near the percolation threshold by mathematical modeling. Tunneling effect theory and Ohm's law are employed in the modeling procedure. To verify the numerical simulation, experiments have also been conducted on CFRC composites that are in the dry state to avoid the influence of ionic conduction.

2. Experimental method

2.1. Raw materials and composite fabrication

The carbon fibers were isotropic PAN-based, unsized, with length of 5 mm, as obtained from SGL Carbon Co. (SGL, Germany). The fiber properties are shown in Table 1. Ordinary Portland cement which corresponds to ASTM Type I was used throughout. The sand used was local natural sand with specific gravity of 2.65. Silica fume (together with a defoamer and a water reducing

* Corresponding author.
E-mail address: 0610060014@tongji.edu.cn (J. Xu).

0958-9465/$ - see front matter © 2010 Elsevier Ltd. All rights reserved.
doi:10.1016/j.cemconcomp.2010.10.007

Nomenclature

V	measured voltage applied on the specimen (V)
I	measured current passing the specimen (A)
ξ	intensity of the applied electric field (V/m)
A	cross-section area of the specimen (m^2)
L	length of the specimen (m)
V_0	volume fraction of carbon fibers (%)
ρ	total resistivity of the specimen (Ω m)
ρ_t	resistivity of the specimen correlates with tunneling effect in a given electric field (Ω m)
ρ_0	resistivity of the specimen correlates with tunneling effect without applied electric field (Ω m)
ρ'	resistivity of the specimen irrelevant to tunneling effect (Ω m)
q	electrostatic capacity of the charge carrier (C)
σ_t	electric conductivity of the specimen correlates with tunneling effect (S/m)
v_d	velocity of charge carriers (m/s)
μ	mobility of charge carriers (m^2/(V s)
m	mass of the charge carrier (kg)
E_V	kinetic energy of the charge carrier (J)
E_0	energy of the charge carrier free from electric field (J)
E_ξ	energy of the charge carrier in a given electric field of intensity ξ (J)
T	transmission probability
N_0	number of barriers connected in series
a	width of the barrier (m)
U_0	height of the barrier (eV)
$\hbar$	reduced Plank's constant (J s)
n	number of charge carriers which can hop across barriers successfully
n_0	total number of charge carriers
i	plural symbol
K	symbol assigned for a constant quantity
λ	the proportion of tunneling effect in influencing the total resistivity

agent [WR]) was used along with fibers. The silica fume (Elkem Materials) was used in the amount of 15% by mass of cement. The defoamer, used in the amount of 0.13 vol.%, was Tri-Butyl-Phosphate. The WR (Kao Chemical Corp., 21s; polycarboxylic type water-reducer) was used in the amount of 1.0% by mass of cement. Water/cement (w/c) ratio was 0.45 (by mass) and sand/cement (s/c) ratio was 1.0 (by mass).

Specimens containing 0.05%, 0.10%, 0.15%, and 0.20% by volume of fibers were prepared under laboratory conditions. A rotary mixer with a flat beater was used for mixing. Fibers were added in water and then the defoamer was added and mixed for about 1 min. Then the mixture, cement, sand, silica fume and WR were mixed in the mixer for 3 min. After pouring into molds, an external vibrator was used to facilitate compaction and decrease the amount of air bubbles. The specimens were demolded after 24 h and then cured in a moist-curing room for 27 days. In order to make sure the completely dry state, all the specimens were heated to 105 °C for 6 h and then put in a desiccator at room temperature.

2.2. Testing

Alternating current (AC) is often used in the measurement of electrical conductivity for the purpose of avoiding the problem of polarization, due to charge carriers moving back and forth as the voltage polarity changes under AC condition [12,13]. However, direct current (DC) is simpler and less expensive than AC. Furthermore, the majority of prior works on CFRC used DC with the well-known four-probe method, as the electrical contact resistance and polarization problem both can be eliminated [14,15].

DC electrical conductivity measurement is performed by using the four-probe method and the configuration is illustrated in Fig. 1. Two Fluke 89 multimeters were used. The specimen was a rectangular bar of size 40 mm × 40 mm × 160 mm. It consisted of the silver coating on both of the two 40 mm × 40 mm sides. Electrical contacts in the form of silver coating in conjunction with copper wire were applied on the side surface and around the entire 40 mm × 40 mm perimeter of the bar. Three specimens of each composition were tested.

During testing, the current and voltage values were recorded at the same time and then converted into resistance by numerical program. The electric field intensity ξ is given by:

$$\xi = \frac{V}{L} \tag{1}$$

where V is the measured voltage applied on the specimen, L is the length of the specimen. The total resistivity ρ would be:

$$\rho = \frac{VA}{IL} \tag{2}$$

where A is the cross-section area of the specimen, I is the measured current passing the specimen.

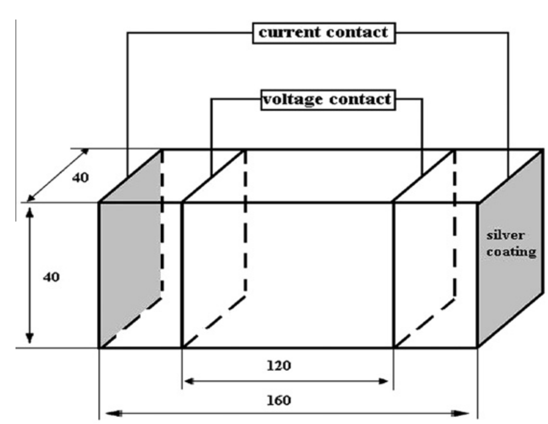

Fig. 1. DC electrical conductivity measurement configuration (mm).

Table 1
Properties of carbon fiber.

Diameter (μm)	Density (g cm^{-3})	Tensile strength (GPa)	Young's modulus (GPa)	Elongation at break (%)	Carbon content (w_c%)	Electrical resistivity (μΩ m)
7 ± 0.2	1.78	>3.0	220–240	1.25–1.60	>95	15

3. Results and discussion

Fig. 2 presents a typical plot of the resistivity vs. voltage for CFRC with 0.05 vol.% fiber content under the condition of small voltage signal. A flat zone appears below 2 V and the resistivity decreases dramatically beyond 2 V. The voltage at which the resistivity starts to deviate from the flat zone is hereby referred to as the critical voltage. The shape of the curve is similar for all fiber fractions, though the values of the critical voltage differ, as listed in Table 2. The marked decreasing of resistivity may be attributed to tunnel transmission of charge carriers which gain the energy from applied electric power.

The probability of neighboring fibers meeting the condition necessary for tunnel transmission relates to the aspect ratio of fibers, which in turn determines the critical volume fraction for percolation. Suppose the fibers are randomly oriented overlapping ellipsoids of revolution with an aspect ratio of 700:1, which is roughly equal to that of the fibers considered in this study. If these are placed in a three-dimensional cell of cement matrix, the critical volume fraction would be around 0.1 vol.% [16]. Thus it is evident that the volume fractions involved in this work are near the percolation threshold and tunnel transmission is highly likely to occur due to the tendency of neighboring fibers to be in near contact. Fig. 3a is a SEM image of two adjacent fibers distributed in the cement matrix but not in contact. Fig. 3b is a magnification (10×) of a portion of Fig. 3a, in which it can be seen that the distance between the two neighboring fibers is within the range of nanometer-scale. This is a prerequisite for tunnel transmission [17,18].

Now considering the CFRC conductive system in an electric field with field intensity ξ, the charge carrier would obtain velocity v_{d}, whose direction is related to the electric field. The velocity vector $\boldsymbol{v_d}$ can be given by the following expression:

$$v_{\mathbf{d}} = \mu\xi \tag{3}$$

where μ is the mobility of charge carriers and can be regarded as constant. From an energy point of view, the charge carrier gains an extra kinetic energy E_v, which can be written as:

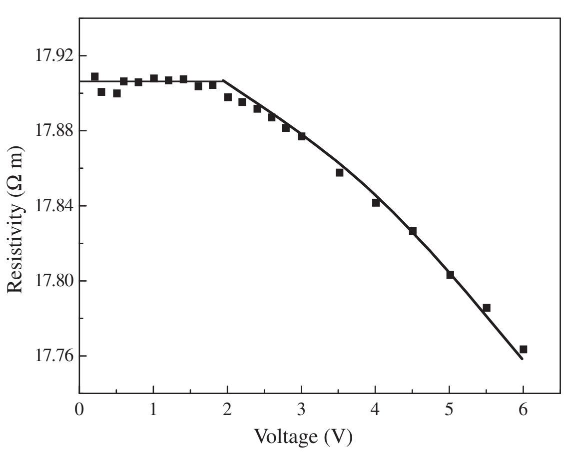

Fig. 2. Resistivity vs. voltage for CFRC with fiber content of 0.05 vol.% under the condition of small voltage.

Table 2
Critical voltage and corresponding resistivity of CFRC.

Fiber content (vol.%)	Critical voltage (V)	Resistivity (Ω m)
0.05	2.10 ± 0.27	17.87 ± 1.07
0.10	1.21 ± 0.09	2.67 ± 0.13
0.15	0.78 ± 0.07	1.51 ± 0.11
0.20	0.45 ± 0.08	1.21 ± 0.13

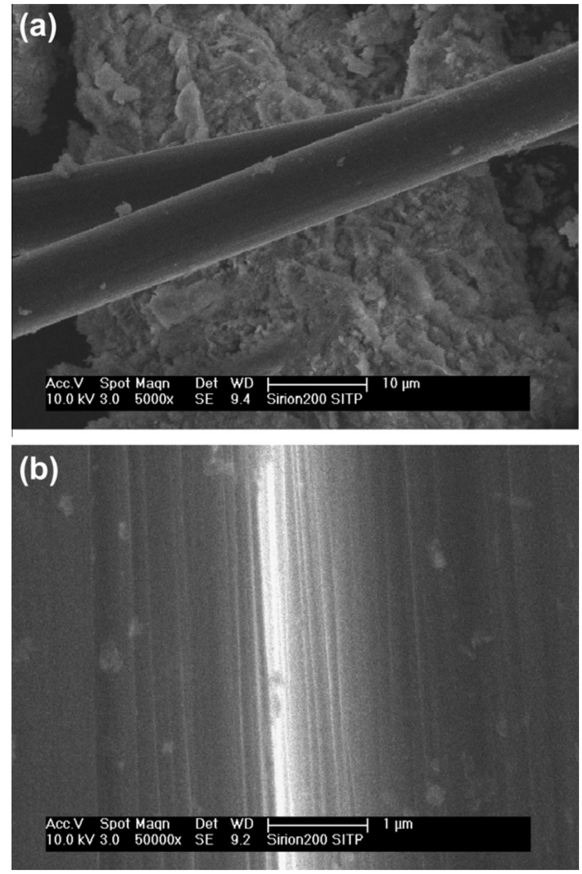

Fig. 3. SEM images of carbon fibers in cement matrix: (a) two adjacent fibers; (b) enlarged view of fiber spacing.

$$E_v = \frac{1}{2}mV_d^2 \tag{4}$$

Let the energy of the charge carrier in the electric field be E_ξ and it should be:

$$E_\xi = E_0 + E_V \tag{5}$$

where E_0 is the energy of the charge carrier free from electric field. Substituting Eqs. (3) and (4) into Eq. (5) results in the following expression:

$$E_\xi = E_0 + \frac{1}{2}m\mu^2\xi^2 \tag{6}$$

For a conductive system, the amount n of charge carriers that can hop across the barrier successfully is given by the expression as follow [19,20]:

$$n = n_0T^{N_0} = n_0\left|\frac{2ik_1}{ik_1 - k_2}\right|^{2N_0} \cdot \exp\left[-\frac{2a}{\hbar}N_0\sqrt{2m(U_0 - E_\xi)}\right] \tag{7}$$

where

$$k_1 = \frac{2mE_\xi}{\hbar^2} \tag{8}$$

$$k_2 = \frac{2m(U_0 - E_\xi)}{\hbar^2} \tag{9}$$

where n_0, T, N_0, U_0, a and $\hbar$ are the total number of charge carriers, transmission probability, number of barriers connected in series, height of the barrier, width of the barrier and reduced Plank's constant, respectively. Substituting Eqs. (8) and (9) into Eq. (7) and then differentiating n with respect to ξ generates:

$$\frac{dn}{d\xi} = nN_0\left(\frac{1}{E_\xi} + \frac{2am}{\hbar\sqrt{2m(U_0 - E_\xi)}}\right)m\mu^2\xi \tag{10}$$

From Eq. (10) it is found that if $\xi > 0$, then $\frac{dn}{d\xi} > 0$.

Under the condition of field intensity not high enough, we have:

$$\frac{1}{2}m\mu^2\xi^2 \ll E_0, \quad \frac{1}{2}m\mu^2\xi^2 \ll (U_0 - E_0) \tag{11}$$

Thereby

$$\frac{1}{E_\xi} \approx \frac{1}{E_0}, \quad \frac{2am}{\hbar\sqrt{2m(U_0 - E_\xi)}} \approx \frac{2am}{\hbar\sqrt{2m(U_0 - E_0)}} \tag{12}$$

Then Eq. (10) can be rewritten as:

$$\frac{dn}{d\xi} = nN_0\left(\frac{1}{E_0} + \frac{2am}{\hbar\sqrt{2m(U_0 - E_0)}}\right)m\mu^2\xi \tag{13}$$

On the other hand, according to Ohm's law, the tunnel transmission resistivity ρ_t of CFRC can be given by:

$$\rho_t = \frac{1}{\sigma_t} = \frac{1}{nq\mu} \tag{14}$$

where σ_t is the conductivity of the specimen correlates with tunneling effect, q is the electrostatic capacity of the charge carrier. Differentiating ρ_t with respect to ξ based on Eqs. (13) and (14) results in:

$$\frac{d\rho_t}{d\xi} = -\frac{1}{\sigma_t^2}\frac{d\sigma_t}{d\xi} = -\frac{1}{n^2q\mu}\frac{dn}{d\xi}$$
$$= -\frac{m\mu^2N_0}{nq\mu}\left(\frac{1}{E_0} + \frac{2am}{\hbar\sqrt{2m(U_0 - E_0)}}\right)\xi \tag{15}$$

Eq. (15) can be simplified as:

$$\frac{d\rho_t}{d\xi} = -2\rho_t K\xi \tag{16}$$

where

$$K = \frac{m\mu^2N_0}{2}\left(\frac{1}{E_0} + \frac{2am}{\hbar\sqrt{2m(U_0 - E_0)}}\right) \tag{17}$$

Integrating the two sides of the equal sign in Eq. (16) produces another form of ρ_t varying with ξ, i.e.,

$$\rho_t = \rho_0 e^{-K\xi^2} \tag{18}$$

where ρ_0 is the resistivity of the specimen related to tunneling effect without applied electric field. The total resistivity ρ would be:

$$\rho = \rho' + \rho_t = \rho' + \rho_0 e^{-K\xi^2} \tag{19}$$

where ρ' is the resistivity resulting from continuous conductive path formed by contact fibers. It is irrelevant to the tunneling effect and can be regarded as constant.

For the purpose of characterizing the impact of field intensity on CFRC resistivity, defining a parameter λ as follow:

$$\lambda = \frac{\rho_0}{\rho' + \rho_0} \tag{20}$$

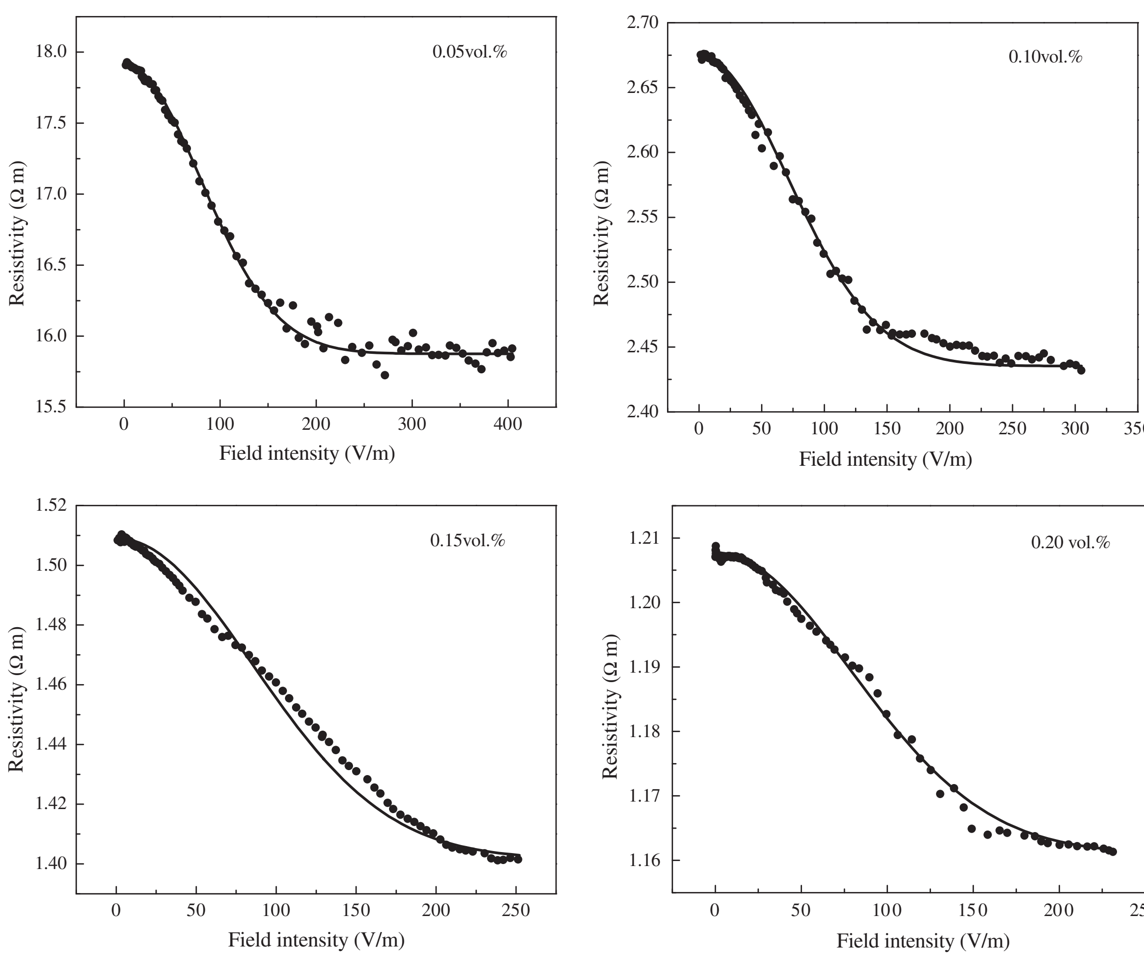

Fig. 4. Plots of resistivity vs. field intensity with four levels of fiber content (solid circles represent experimental results and solid lines represent the fitting curves).

Table 3
Theoretical fitting results for CFRC with different fiber content.

Parameters	Carbon fiber content (vol.%)			
	0.05	0.10	0.15	0.20
ρ' (Ω m)	15.87 ± 0.63	2.43 ± 0.15	1.40 ± 0.06	1.16 ± 0.05
ρ_0 (Ω m)	1.99 ± 0.19	0.23 ± 0.02	0.11 ± 0.01	0.05 ± 0.01
λ (%)	0.111 ± 0.006	0.086 ± 0.004	0.073 ± 0.005	0.041 ± 0.002
K	$(7.91 \pm 0.08) \times 10^{-5}$	$(1.07 \pm 0.03) \times 10^{-4}$	$(7.07 \pm 0.06) \times 10^{-5}$	$(8.03 \pm 0.08) \times 10^{-5}$
r (%)	99.5	99.7	99.9	99.9

Here, λ represents the proportion of tunneling effect in influencing the total resistivity of CFRC. According to the definition of ρ_0, it is obvious that ρ_0 is the maximum value of tunnel transmission resistivity. As the research has shown, whether or not the charge carriers can hop across the tunneling barrier is very sensitive to the variation of fiber content, especially when the fiber content is in the vicinity of the percolation threshold, for the width of barrier depends on the volume fraction of fibers. In other words, ρ_0 decreases dramatically as fiber content increases. However, ρ' almost decreases linearly with increasing fiber content [21]. For the analysis cited above, it is expected that λ will decrease as fiber content increases.

Fig. 4 shows plots of resistivity vs. field intensity of CFRC with different fiber fractions. Tests were carried out on three specimens for each fiber fractions and the data scatter of results is within the range of 10%, indicating that the results were repeatable. Therefore, the results of the replicated specimens are not presented here. The fitting curves, which denoted as the theoretical curves, are also depicted out for comparison. The agreement between the experimental curves and theoretical curves indicates that the analysis of the relationship between the resistivity and the electric field intensity involving tunneling effect is reasonable. Fitting results concerning parameters ρ', ρ_0, λ and K are listed in Table 3. Obviously, the corresponding correlation coefficient r for each fiber fraction is close to 100%, which further confirms the rationality of the proposed model. For all fiber fractions, ρ', ρ_0 and λ are decreased along with increasing fiber content. The descending trend of λ indicates that the influence of electric field intensity on the resistivity related to tunneling effect has been significantly weakened due to the increasing fiber content. Thus the tunneling barrier does not hinder the motion of charge carriers anymore when the fiber content approaches percolation threshold and ohmic continuum conduction is dominant for the conduction of system.

4. Conclusion

Nonlinear *I–V* behavior was found to be a typical characteristic of CFRC near the percolation threshold. A flat zone appears when the applied voltage is very low and the critical voltage beyond which the resistivity starts to drop dramatically differs with varying fiber content. Modeling on the conductive mechanism of CFRC was carried out using tunneling effect theory and Ohm's law. The corresponding mathematical model was validated through comparisons with experimental results. Results also show that the resistivity related to tunneling effect and its proportion in the total resistivity decrease simultaneously along with increasing fiber content. Tunneling effect becomes negligible when fiber fractions are in the vicinity or above the percolation threshold. The model provides information for the practical application of CFRC and it is potentially helpful in engineering CFRC with improved properties.

Acknowledgements

The authors would like to acknowledge the financial support for this study from the National Natural Science Foundation of China (No. 50238040) and the Program for Young Excellent Talents in Tongji University.

References

[1] Amaral V, Araújo J, Lourenco A, Tavares P, Pogorelov Y, Sousa J, et al. Non-linear conduction in $LaCaMnO_3$ thin films: interface tunneling effects. J Magn Magn Mater 2001;226–230:942–4.
[2] Radhakrishnan S, Kar S. Role of non-linear processes in conducting polymer blends for piezo-sensors part 2: studies on polyaniline/SBS blends. Sens Actuators, A 2005;120:474–81.
[3] Clarke D. Application of zinc oxide varistors. J Am Ceram Soc 1999;82: 485–502.
[4] Li H, Xiao H, Ou J. Effect of compressive strain on electrical resistivity of carbon black-filled cement-based composites. Cem Concr Compos 2006;28:824–8.
[5] Wen S, Chung DDL. Carbon fiber-reinforced cement as a thermistor. Cem Concr Res 1999;29:961–5.
[6] Hixson A, Woo L, Campo M, Mason T. The origin of nonlinear current–voltage behavior in fiber-reinforced cement composites. Cem Concr Res 2003;33: 835–40.
[7] Chiarello M, Zinno R. Electrical conductivity of self-monitoring CFRC. Cem Concr Compos 2005;27:463–9.
[8] Chen B, Wu K, Yao W. Conductivity of carbon fiber reinforced cement-based composites. Cem Concr Compos 2004;26:291–7.
[9] Chung DDL. Cement reinforced with short carbon fibers: a multifunctional material. Compos Part B 2000;31:511–26.
[10] Wen S, Chung DDL. The role of electronic and ionic conduction in the electrical conductivity of carbon fiber reinforced cement. Carbon 2006;44:2130–8.
[11] Wen S, Chung DDL. Effect of carbon fiber grade on the electrical behavior of carbon fiber reinforced cement. Carbon 2001;39:369–73.
[12] Woo LY, Wansom S, Ozyurt N, Mu B, Shah SP, Mason TO. Characterizing fiber dispersion in cement composites using AC-impedance spectroscopy. Cem Concr Compos 2005;27:627–36.
[13] Reza F, Yamamuro JA, Batson GB. Electrical resistance change in compact tension specimens of carbon fiber cement composites. Cem Concr Compos 2004;26:873–81.
[14] Wen S, Chung DDL. Electrical-resistance-based damage self-sensing in carbon fiber reinforced cement. Carbon 2007;45:710–6.
[15] Wen S, Chung DDL. Double percolation in the electrical conduction in carbon fiber reinforced cement-based materials. Carbon 2007;45:263–7.
[16] Garboczi EJ, Snyder KA, Douglas JF, Thorpe MF. Geometrical percolation-threshold of overlapping ellipsoids. Phys Rev E 1995;52:819–28.
[17] Sheng P, Sichel EK, Gittleman JI. Fluctuation-induced tunneling conduction in carbon–polyvinylchloride composites. Phys Rev Lett 1978;40:1197–200.
[18] Pikus FG, Likharev KK. Nanoscale field-effect transistors: an ultimate size analysis. Appl Phys Lett 1997;71:1–4.
[19] Robinett RW. Quantum mechanics. Oxford University Press; 1997.
[20] Roland W. Scanning probe microscopy and spectroscopy: methods and applications. Cambridge University Press; 1994.
[21] Dani A, Ogale AA. Electrical percolation behavior of short-fiber composites: experimental characterization and modeling. Compos Sci Technol 1996;56: 911–20.